

Photometric observations of the radio bright B[e]/X-ray binary CI Cam

J.S. Clark¹, A.S. Miroshnichenko^{2,3}, V.M. Larionov⁴, V.M. Lyuty⁵, R.I. Hynes^{6,7}, G.G. Pooley⁸, M.J. Coe⁶, M. McCollough⁹, S. Dieters⁹, Yu.S. Efimov^{10,11}, J. Fabregat¹², V.P. Goranskii⁵, C.A. Haswell⁷, N.V. Metlova⁵, E.L. Robinson¹³, P. Roche¹⁴, V.I. Shenavrin⁵, and W.F. Welsh¹³

¹ University of Sussex, Astronomy Centre, Falmer, Brighton, BN1 9QH, UK

² Pulkovo Observatory, 196140 Saint-Petersburg, Russia

³ University of Toledo, Dept. of Physics & Astronomy, Toledo, OH 43606, USA

⁴ Astronomical Institute of St. Petersburg University, 198904 St. Petersburg, Russia

⁵ Crimean Laboratory of Sternberg Astronomical Institute of Moscow University, Russia

⁶ University of Southampton, Department of Physics & Astronomy, Highfield, Southampton SO17 1BJ, UK

⁷ The Open University, Department of Physics, Walton Hall, Milton Keynes MK7 6AA, UK

⁸ Mullard Radio Astronomy Observatory, Cavendish Laboratory, Madingley Road, Cambridge CB3 0HE, UK

⁹ NASA/Marshall Space Flight Center, Huntsville, Alabama, AL 35812, USA

¹⁰ Crimean Astrophysical Observatory, Nauchny, Crimea, 334413, Ukraine

¹¹ Isaac Newton Institute of Chile, Crimean Branch

¹² Departamento de Astronomia, Universidad de Valencia, 46100 Burjassot, Valencia, Spain

¹³ Dept. of Astronomy, University of Texas, Austin, TX 78712, USA

¹⁴ NSSC, Mansion House, 41 Guildhall Lane, Leicester, LE1 5FQ, UK

Received 22 December 1999 / Accepted 27 January 2000

Abstract. We present multiwavelength (optical, IR, radio) observations of CI Cam, the optical counterpart to the transient X-ray source XTE J0421+560. Pre-outburst quiescent observations reveal the presence of a dusty envelope around the system. Pronounced short term variability is observed at all wavebands from $U-K$, but no indication of prior flaring of a similar magnitude to the 1998 April outburst is found in these data.

Data obtained during the 1998 April X-ray flare reveal pronounced optical-radio flaring. The optical flux was observed to quickly return to quiescent levels, while the radio flare was of much longer duration. The optical component is likely to result from a combination of free-free/free-bound emission, emission line and thermal dust emission, caused by re-radiation of the X-ray flux, while the behaviour of the multiwavelength radio data is consistent with emission from expanding ejecta emitting via the synchrotron mechanism.

Post-outburst (1998 August–1999 March) $U-M$ broadband photometric observations reveal that while the optical (UBV) flux remains at pre-outburst quiescent levels, near IR ($JHKLM$) fluxes exceed the pre-outburst fluxes by ~ 0.5 magnitudes. Modelling the pre- and post-outburst spectral energy distribution of CI Cam reveals that the structure and/or composition of the dusty component of the circumstellar envelope appears to have changed. Due to a lack of information on the precise chemical composition of the dust within the system several explanations for this behaviour are possible, such as the produc-

tion of new dust at the inner edge of the envelope, or modification of the composition of the dust due to X-ray irradiation.

Key words: stars: binaries: general – stars: circumstellar matter – stars: individual: CI Cam – stars: winds, outflows – X-rays: stars

1. Introduction

The bright X-ray transient XTE J0421+560 was first detected by the Rossi X-Ray Timing Experiment (RXTE) All-Sky Monitor, with the onset of the flare on 1998 March 31, and the peak in flux on 1998 April 1 (JD 2450905) in the 2–12 keV band (Smith et al. 1998). Emission at energies of up to 70 keV was also detected by the Burst and Transient Source Experiment (BATSE; Harmon et al. 1998) experiment aboard the Compton Gamma Ray Observatory (CGRO; Fishman et al. 1989). The source was observed to fade quickly, with an initial e-folding time of ~ 0.5 days (Belloni et al. 1999; henceforth B99). The X-ray spectrum was found to be consistent with both thermal (Ueda et al. 1998) and non-thermal interpretations with evidence for variable intrinsic absorption during the outburst (B99, Orr et al. 1998). The bright ($V \sim 11$) B[e] star CI Cam (=MWC 84) was found to lie near to the centre of 1' radius error circle determined from PCA RXTE observations (Marshall & Strohmayer 1998). Spectroscopic observations of CI Cam by Wagner et al. (1998) on 1998 April 3 revealed a rich emission line spectrum with He II in emission. These features had been absent from

Send offprint requests to: J.S. Clark

Correspondence to: (jsc@star.cpes.susx.ac.uk)

Table 1. Summary of observations giving details of telescope and detector used, photometric bands observed in and dates of observations. Note the following abbreviations have been employed: JKT–Jakobus Kapteyn Tel.; CLSAI–Crimean Laboratory of SAI; SPb–St.Petersburg University; CrAO–Crimean Astrophys. Obs.;McD–McDonald Obs.; T-Sh–Tien-Shan Obs.; TCS–Telescope Carlos Sanchez.

| Observatory | Size(m) | Date | Detector | Bands |
|-------------|---------|-------------------|------------------|-----------|
| JKT | 1.00 | Apr.1998 | TEK4 CCD | UBVRI |
| CL SAI | 0.60 | Apr.1998 | EMI 9789, ST-6UV | UBVRI |
| CL SAI | 1.25 | Dec.1998-Sep.1999 | InSb | JHKLM |
| SPb | 0.70 | Aug.1998-Sep.1998 | InSb | JHKLM |
| SPb | 0.20 | Mar.1999 | CCD | BVRI |
| CrAO | 1.25 | Sep.1998-Jan.1999 | photomult. | UBVRI |
| McD | 0.90 | Apr.1998 | White Guider CCD | no filter |
| McD | 2.10 | Apr.1998 | White Guider CCD | no filter |
| McD | 2.70 | Apr.1998 | CCD | UBVRI |
| T-Sh | 1.00 | Aug.1998-Mar.1999 | photomult., PbS | UBVRIJHK |
| TCS | 1.50 | Oct.1998-Oct.1999 | CVF | JHK |

previous spectra (Downes 1984), and by analogy with other X-ray Binaries CI Cam was proposed as the optical counterpart to J0421+560 (Wagner et al. 1998). On 1998 April 1 Hjellming & Mioduszewski (1998a) detected a transient 1.4 GHz source with a flux of 19 mJy coincident with the optical position of CI Cam, thus confirming the identification of CI Cam as the optical counterpart. The discovery of rapid radio variability established that the emission was of non thermal (synchrotron) origin (Hjellming & Mioduszewski 1998b).

In this paper we present broadband *UBVRIJHKLM* photometric observations of CI Cam obtained between 1989–1999. We compare the optical-IR behaviour to the X-ray and radio lightcurves of the source during the X-ray outburst. We use the pre-outburst data from Bergner et al. (1995) to define a mean quiescent state for CI Cam and model both pre- and post-outburst data, in conjunction with IRAS photometry between 12–60 μm and an IRAS LRS spectrum, with the code DUSTY (Ivezić et al. 1999). Finally we investigate the properties of the increased IR emission present in the system since the 1998 outburst.

2. Data reduction and flux calibration

UBVRIJHKLM photometry has been obtained from a number of instruments both during and after the 1998 April X-ray -radio flare. *UBVRI* photometry was obtained from the 1.0 m Jakobus Kapteyn Telescope (JKT) on La Palma, the 0.6m and 1.25 m telescopes of the Crimean Laboratory of Sternberg Astronomical Institute (CL SAI), the 1.25 m telescope of the Crimean Astrophysical Observatory (CrAO) and the 0.9 m and 2.1 m telescopes at McDonald Observatory (McD). Data from CL SAI were obtained with an ST-6UV CCD and pulse counting photometer with an EMI 9789 photomultiplier, and filter set consistent with the Johnson system. All measurements made at the CrAO were carried out with the double beam five channel computer-controlled photopolarimeter developed in Helsinki University (Finland) by Pirola (1988). Additional *BVRI* observations were obtained with the 0.2 m telescope of St.Petersburg University (SPb) with a ST-8 CCD, using a Cousins filter set. JKT observations were made with the TEK4 CCD camera mounted at the Cassegrain focus, using the Harris

UBVRI filter set and McDonald observations with the White Guider CCD camera, with observations on 1998 April 15.1 and 17.1 using the 0.9 m telescope and those on April 19.1 and 20.2 using the 2.1 m.

Simultaneous Johnson *UBVRIJHK* photometry was obtained at the 1.0 m telescope of the Tien-Shan Observatory (T-Sh; Fesenkov Astrophysical Institute, Kazakhstan) with a two-channel photometer-polarimeter of the Pulkovo Observatory equipped with a thermoelectrically cooled GaAs photomultiplier and a PbS detector (Bergner et al. 1988).

JHKLM photometry was obtained from the Telescope Carlos Sanchez (TCS), Tenerife, the 1.25 m telescope at CL SAI, and the 0.7 m telescope at SPb. TCS data were acquired with the CVF detector and CL SAI and SPb data with an InSb liquid nitrogen cooled photodiode photometer. These observations are summarised in Table 1. Additional outburst photometry were obtained from Robinson et al. (1998), Garcia et al. (1998) and VSNET observations. The Johnson filter system was assumed as the default for VSNET observations; we note that this approximation does not affect our conclusions (the data are plotted only in Fig. 1, and not analysed further). Eq. (1) and the calibration constants, C_λ , given in Telting et al. (1998) and reproduced in Table 2 were employed for conversions between magnitude and fluxes.

$$\log F_\nu = -0.4m_\lambda - C_\lambda \quad (1)$$

15 GHz radio observations of CI Cam were made from the Ryle Telescope, and were reduced following the method detailed in Pooley & Fender (1997), using B0415+572 as a phase calibrator, and the flux density determined from observations of 3C 48 and 286. 8.3 & 2.25 GHz observations were obtained from the public access lightcurves of the NRAO/NASA GBI telescope (eg Waltman et al. 1994, Frontera et al. 1998; henceforth F98).

3. Radio observations

Table 2. Calibration constants, C_λ , used to convert magnitudes to fluxes in $\text{erg/cm}^2/\text{s/Hz}$, using $\log F_\nu = -0.4m_\lambda - C_\lambda$.

| Filter System | U | B | V | R | I | J | H | K | L | M |
|---------------|--------|--------|--------|--------|--------|--------|--------|--------|--------|--------|
| Johnson | 19.764 | 19.348 | 19.436 | 19.556 | 19.650 | 19.802 | 19.996 | 20.200 | 20.562 | 20.807 |
| Crimean | 19.743 | 19.388 | 19.426 | 19.548 | 19.648 | 19.795 | 19.983 | 20.166 | 20.551 | 20.794 |
| Cousins | 19.742 | 19.371 | 19.439 | 19.511 | 19.593 | | | | | |
| TCS | | | | | | 19.804 | 20.007 | 20.179 | | |

3.1. Pre-outburst observations

Several radio observations of this region of sky had been made prior to 1998. Observations made at 10.6 GHz in 1973 May and July provide upper limits of 25 mJy (Altenhoff et al. 1976) and 5mJy (Woodsworth & Hughes 1977) respectively. The 87GB survey by Gregory and Condon (1991) provided an upper limit to the 4.85 GHz flux of 25 mJy in 1987 October. The 7C survey at 151 MHz gives a 5σ limit of 150 mJy in 1993 November (Vessey & Green 1998), while the NVSS shows no evidence of emission at 1.4 GHz, implying an upper limit of ~ 1 mJy on 1994 January 18–19 and 21–22 (J. Condon, priv. comm.). Unfortunately there are no other contemporaneous data to determine if the system was in a ‘quiescent’ or ‘active’ state during these observations.

3.2. Outburst observations

The 15, 8.3 and 2.25 GHz radio lightcurves are reproduced in Fig. 1; their behaviour can be explained in terms of the evolution of an expanding shell of ejecta emitting via the synchrotron mechanism. The ejecta are optically thin at 15 & 8 GHz in all observations, but show a transition between optically thick and thin emission at 2 GHz between JD 2450907–09 (1998 April 3–5). In the simple model of synchrotron emission from an expanding source of van der Laan (1966), the maximum flux density observed at a given frequency occurs just before the transition to the optically thin regime; as the opacity has a λ^2 dependence one expects the peak flux at a given wavelength to be delayed relative to emission at shorter wavelengths, as is indeed seen. Further, detailed analysis of these data will be presented by Hjellming et al. (in prep.); therefore we refrain from further discussion here.

The fluxes at all three wavelengths continued to fall (Hjellming et al.; in prep), and by \sim JD 2451100 (October 13) both the 2 & 8 GHz flux had fallen below the detection threshold of the GBI (~ 10 mJy). Further observations of the 15 GHz flux until 1999 October indicate the flux has continued to decrease monotonically (Fig. 5). There is no indication of significant flaring in this data set around or after JD 2451232–2451245 (1999 February 22–March 7), when BATSE detected a marginal X-ray flare in the 20–100 keV band (see Sect. 4.4). We note that on two occasions the 8 GHz GBI flux increased for a few days (JD 2451185–2451201 and JD 2451235–2451242; 1999 January 10–26 and February 26–March 5 respectively), the latter such ‘flare’ coinciding with the 20–100 keV flaring observed by BATSE. However, after consulting the observing log we note

that these two periods corresponded to increased system noise temperatures, and we believe that they should be discounted.

4. Optical-IR broadband photometry

4.1. Pre-outburst observations: 1970–1992

Broad band photometric measurements dating from the early 1970’s of $V=11.4$, $H=6.14$ and $K=5.0$ are reported by Allen & Swings (1976). IRAS observations provide fluxes of 8.23 Jy, 2.84 Jy and 0.76 Jy at 12, 25 and 60 microns respectively; the optical-IRAS spectral energy distribution (SED), is indicative of emission from hot dust, and is shown in Fig. 7.

Bergner et al. (1995) report long term *UBVRIJHK* observations made between 1989–1992. Variability on day to day timescales, with an amplitude of ~ 0.4 mag, was observed in all wavebands over this period at greater than the 5σ level. Miroshnichenko (1995) performed a Fourier analysis of these data and identified a quasi-period of 11.7 days, which he interpreted as a possible binary orbital period. Colour/magnitude plots of these data are presented in Figs. 2 and 3. and discussed in Sect. 5.1.1.

4.2. Outburst Observations: 1998 April

Multiwavelength lightcurves covering the outburst are shown in Fig. 1; it is immediately apparent that a large optical-radio outburst has accompanied the X-ray flare. Due to the delay in associating the X-ray transient with CI Cam, the lightcurve is poorly sampled before 1998 April 3, with just one R band observation during this time, and thus it is not possible to determine if the peak in optical-radio flux is displaced from the peak in the X-ray flux. Unfortunately no reliable near-IR photometry of the source was obtained during the outburst. However, *JHK* spectra obtained on April 5–6 clearly indicate the presence of a substantial near IR flaring component at this time (B99), which they attribute to heating of the circumstellar dust.

The decline in flux evident in the *UBVRI* lightcurves (see also Goranskii et al. 2000) is consistent with the exponential decay reported by other workers at other wavelengths (eg F98, B99). Decay rates for the CL SAI *BVR* lightcurves between 1998 April 3–10 give a mean e-folding time of $\sim 3.4 \pm 0.4$ days, while those obtained between April 15–20 (McD data set) showed that the decay rate had fallen significantly, with a mean e-folding rate of ~ 24 days at this time. The mean value obtained between April 3–10 is consistent with optical and 8 GHz radio decay rates determined for the same time period by F98. Additionally, it is marginally consistent with that measured

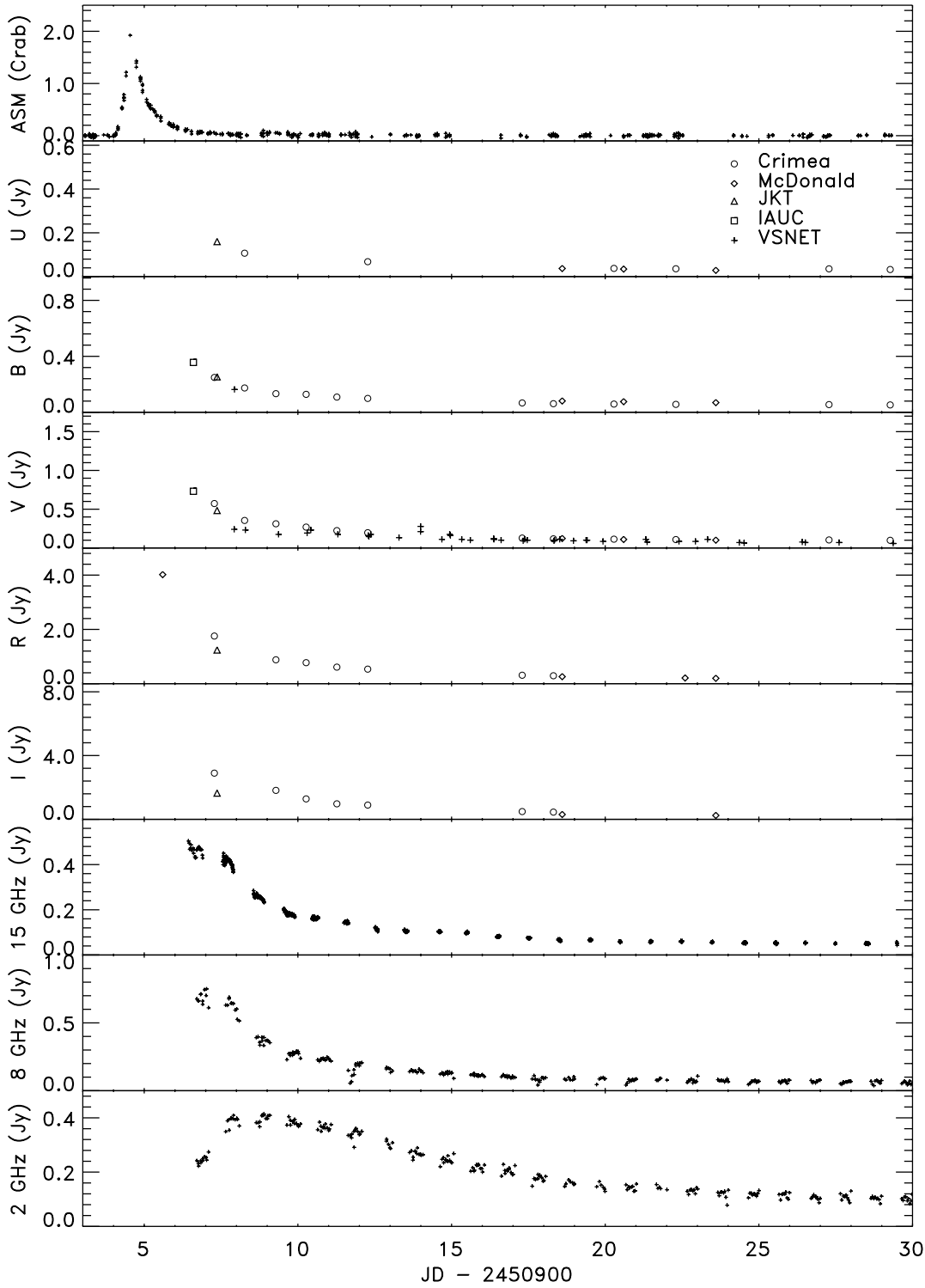


Fig. 1. X-ray - radio outburst lightcurves from 1998 April; note that no dereddening has been applied to the data. The different sources of data are indicated by the use of differing symbols; the key is provided in panel 2.

for the BeppoSAX 1.5–10 keV band flux (2.3 ± 0.3 ; 2σ difference), but not with that obtained for the 0.3–3 keV band flux ($\tau = 1.2 \pm 0.2$ days; 5σ difference) (F98).

We find a very strong linear correlation during the decay phase of the outburst in the broadband *BVRI* fluxes during the outburst, and also with the 15 & 8 GHz radio flux (Fig. 1).

The correlation between the optical (*BVRI*) and 2 GHz flux is weaker, due to the relatively late peaking of the 2 GHz flux (due to the greater optical depth at this wavelength; Sect. 3). Given that the spectral index inferred from the radio data would imply a much greater optical flux than is observed (after correction for interstellar reddening; see Sect. 5.0), it appears unlikely that the

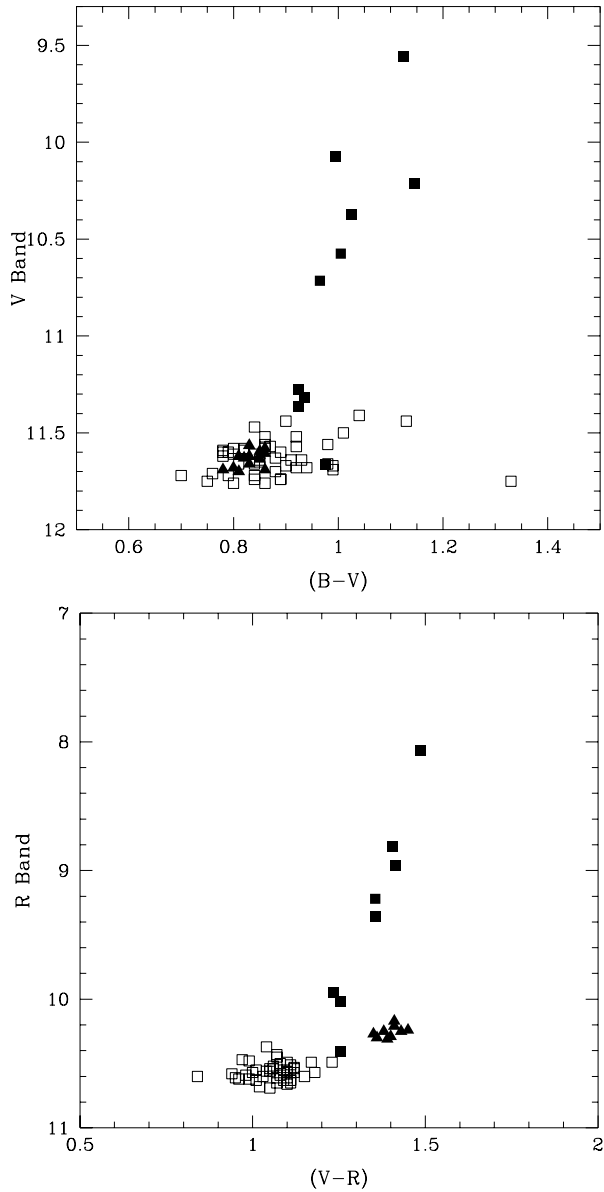


Fig. 2. Optical Colour/Magnitude plots for CI Cam showing quiescent (1989–1992; open squares), outburst (1998 April; solid squares), and post-outburst (1998 August–solid triangles) observations. Note the offset of post-outburst points in the $(V-R)/R$ plot due to the increased R band emission; we interpret this as an increased contribution from gaseous thermal emission ($f-f/b-f$ and recombination line).

optical emission is due to synchrotron emission, as is inferred for the radio emission. Unlike F98 we find evidence for a significant reddening of the system at this time in the $(B - V)/V$ and $(V - R)/R$ colour/magnitude plots (Fig. 2). Although the data are sparse, there appeared to be no significant change in colour in the $(U - B)/B$ colour magnitude plot (not shown). These relationships, and the possible sources of emission are discussed in Sect. 5.1.2.

F98 report flickering in broadband V and R photometry obtained on 1998 April 6, with an amplitude of ~ 0.3 mag on

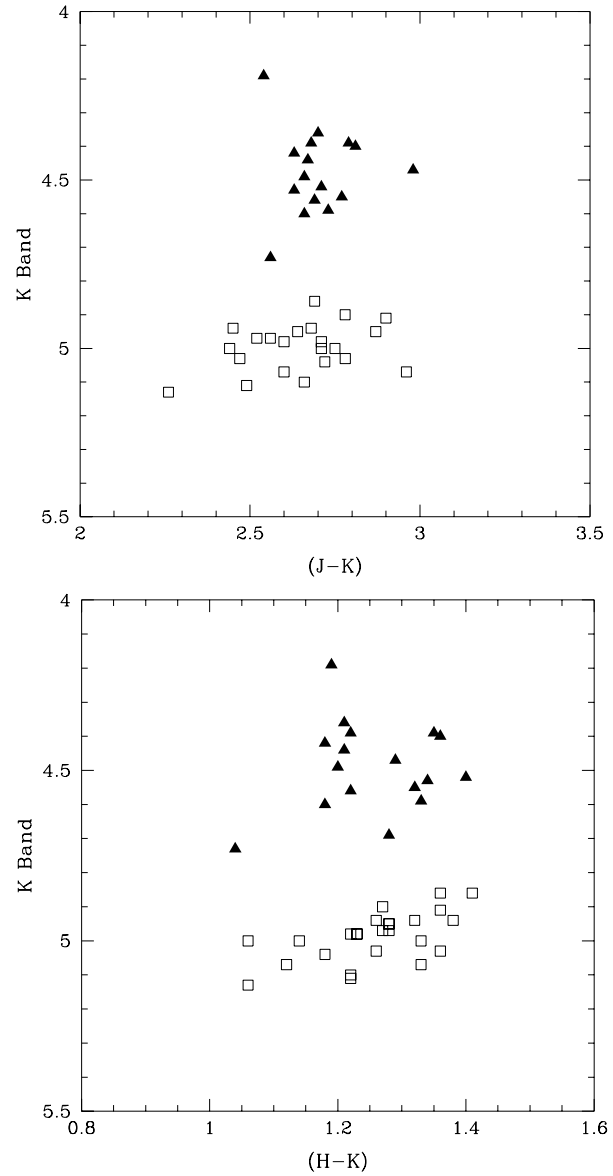


Fig. 3. Near IR Colour/Magnitude plots for CI Cam showing quiescent (1989–1992; open squares) and post-outburst (1998 August–solid triangles) observations. In both plots there is a significant increase in post-outburst emission, probably due to increased thermal dust emission.

timescales of ~ 1 hour, but find no further variability at later times. Observations on 1998 April 13 with the McD 0.92m McD telescope and an unfiltered PMT provided an upper limit to variability of < 1 per cent rms between $1800s > t > 10s$ on that date. Subsequently, we obtained further time series photometry of CI Cam on several separate occasions to search for variability. On 1998 April 19.1 observations were made with the White Guider CCD camera on the 2.2m telescope at McDonald Observatory, Texas. 72 consecutive 1.5-s exposures were taken in the R band spanning 36-min. Standard IRAF data reduction procedures and aperture photometry were used to obtain absolute instrumental magnitudes (no sufficiently bright comparison star was avail-

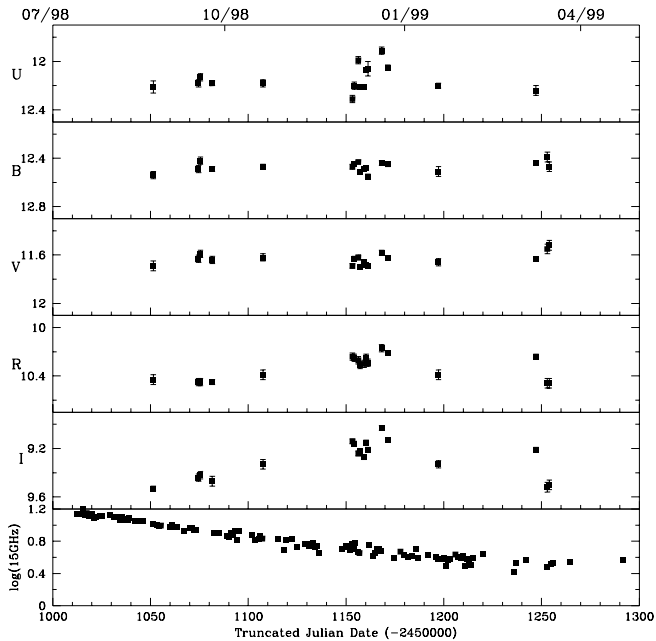


Fig. 4. Post-outburst broadband *UBVR* lightcurves for CI Cam. Note that for most points the errors are smaller than the symbol size. The 15 GHz (Ryle) radio lightcurve has been presented in the bottom panel for comparison; note the clear lack of correlation between radio and optical fluxes (15 GHz data presented in $\log(\text{mJy})$).

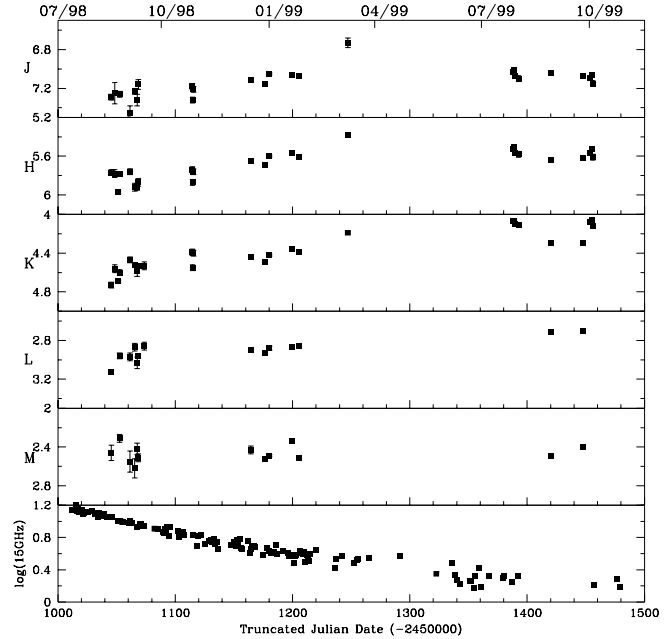


Fig. 5. Post-outburst broadband *JHKLM* lightcurves for CI Cam. Note that for most points the errors are smaller than the symbol size. The 15 GHz (Ryle) radio lightcurve has been presented in the bottom panel for comparison; as with the optical data there is no correlation between radio and near-IR fluxes (15 GHz data presented in $\log(\text{mJy})$). Please note the longer baseline of near-IR observations (~ 15 months) compared to optical observations (~ 9 months).

able). However, no variability was found to be present at a level greater than 1 percent. CI Cam was subsequently observed twice more with a high-speed photometer in white light (3500 to 6000 Å) on the 0.92-m telescope at McDonald Observatory for two hours on October 28 and four hours on October 29 (UTC) to search for periodic variations in the post-outburst light curve. No *periodic* variability between $1000\text{s} > t > 2\text{s}$ was observed to limits of <0.07 per cent (October 28) and <0.05 per cent (October 29) of the continuum flux at this time.

4.3. Post-outburst observations: 1998 August–1999 February

Broadband photometry (*UBVRJHKLM*) was obtained from a number of sites in the period 1998 August–1999 March and is presented in Tables 3 and 4, and Figs. 4 and 5. There is no evidence for significant optical emission in excess of the pre-outburst flux, indeed it is possible that CI Cam is marginally fainter in the *U* band than the mean of the 1990–94 data. Mean *B* and *V* band magnitudes differ little, if at all from the pre-outburst means; the data also lie in the same region of the magnitude/colour plot (Fig. 2), and demonstrate the same ~ 0.4 mag colour independent fluctuations as the pre-outburst data. There is some indication of increased variability in the *U* band during 1998 December; however this is not seen in the *B* & *V* bands. If this is indicative of variable emission from a hot component within the system, such as an accretion disc or an irradiated body we might expect increased X-ray emission at this time; however this is not observed.

However, a significant excess in emission over the pre-outburst data is seen longwards of the *V* band (eg Figs. 3 and 5); the lack of correlation between the *RI* and *JHKLM* bands suggesting emission from two or more components. The first post-outburst observations, obtained ~ 4 months after the X-ray outburst indicated that CI Cam was ~ 0.2 mag. brighter than the mean quiescent value in *R*, and ~ 0.4 mag. brighter in *JHKLM*. The *RIJHK* magnitudes were observed to increase monotonically, with the *RI* bands fluxes reaching a maximum during 1998 December, and the *JHK* bands peaking in 1999 March. Following these maxima the (somewhat sparse) observations of the *RI* bands indicate a reduction in flux, while the *JHK* fluxes remain \sim constant (Figs. 4 and 5). *L* band fluxes were observed to rise by ~ 0.3 mag. between 1998 August–1999 September, while no overall trend was observed in the *M* band fluxes throughout this period ($\Delta M \leq 0.2$ mag.). There appears to be no correlation between the variations in the $(V - R)$ colour index and *R* band magnitude at this time, although CI Cam is redder than during 1990–94. Likewise, the increase in *JHK* flux is not accompanied by colour changes (Fig. 3).

4.4. A second flaring episode?

Between 1999 February 22–March 9 BATSE detected an enhanced X-ray flux in the 20–100 keV energy range (Fig. 6). The BATSE Large Area Detectors (LADs) can monitor the whole sky almost continuously in the energy range of 20 keV–2 MeV

Table 3. Post-outburst *UBVRI* photometry from 1998 August – 1999 February. Calendar and Truncated Julian Dates are given in Columns 1 and 2. Column 3 indicates the source of the data using the abbreviations given in Table 2. The magnitudes and associated errors for *UBVRI* bands given in Columns 4–7. All data are quoted in the Johnson filter system.

| Date | J.D. -2450000 | Source | U | B | V | R | I |
|--------------|------------------|--------|------------|------------|------------|------------|-----------|
| Mean 1990–94 | - | - | 12.0 | 12.4 | 11.6 | 10.6 | 9.6 |
| 28/08/98 | 1051.46 | T-Sh | 12.21±0.05 | 12.54±0.03 | 11.69±0.04 | 10.43±0.04 | 9.53±0.02 |
| 17/09/98 | 1074.57 | CrAO | 12.18±0.03 | 12.49±0.03 | 11.63±0.03 | 10.45±0.03 | 9.44±0.03 |
| 18/09/98 | 1075.56 | CrAO | 12.13±0.03 | 12.42±0.03 | 11.59±0.03 | 10.45±0.03 | 9.42±0.03 |
| 24/09/98 | 1081.59 | CrAO | 12.18±0.02 | 12.49±0.02 | 11.64±0.03 | 10.45±0.02 | 9.47±0.04 |
| 20/10/98 | 1107.54 | CL SAI | 12.18±0.03 | 12.47±0.02 | 11.62±0.03 | 10.39±0.04 | 9.33±0.04 |
| 05/12/98 | 1153.29 | T-Sh | 12.31±0.03 | 12.47±0.02 | 11.69±0.02 | 10.24±0.03 | 9.14±0.02 |
| 06/12/98 | 1154.25 | T-Sh | 12.20±0.03 | 12.45±0.01 | 11.63±0.02 | 10.25±0.03 | 9.16±0.02 |
| 08/12/98 | 1156.28 | T-Sh | 11.99±0.03 | 12.43±0.01 | 11.62±0.02 | 10.27±0.03 | 9.24±0.02 |
| 09/12/98 | 1157.25 | T-Sh | 12.21±0.01 | 12.51±0.01 | 11.70±0.01 | 10.31±0.03 | 9.22±0.02 |
| 11/12/98 | 1159.27 | T-Sh | 12.21±0.01 | 12.49±0.01 | 11.66±0.01 | 10.20±0.03 | 9.27±0.02 |
| 12/12/98 | 1160.27 | T-Sh | 12.07±0.02 | 12.48±0.01 | 11.68±0.01 | 10.25±0.03 | 9.15±0.02 |
| 13/12/98 | 1161.24 | T-Sh | 12.06±0.06 | 12.55±0.02 | 11.69±0.02 | 10.29±0.03 | 9.21±0.02 |
| 20/12/98 | 1168.23 | T-Sh | 11.91±0.03 | 12.44±0.02 | 11.58±0.02 | 10.17±0.03 | 9.03±0.02 |
| 23/12/98 | 1171.33 | T-Sh | 12.05±0.02 | 12.45±0.02 | 11.62±0.01 | 10.21±0.02 | 9.13±0.02 |
| 18/01/99 | 1197.33 | CrAO | 12.20±0.02 | 12.51±0.04 | 11.66±0.03 | 10.39±0.04 | 9.33±0.03 |
| 09/03/99 | 1247.16 | T-Sh | 12.24±0.04 | 12.44±0.01 | 11.63±0.01 | 10.24±0.02 | 9.21±0.02 |
| 15/03/99 | 1253.00 | SPb | - | 12.39±0.04 | 11.55±0.04 | 10.46±0.04 | 9.52±0.04 |
| 16/03/99 | 1254.00 | SPb | - | 12.47±0.04 | 11.52±0.04 | 10.46±0.04 | 9.50±0.04 |

Table 4. Post-outburst *JHKLM* photometry from 1998 August – 1999 February. Calendar and Truncated Julian Dates are given in Columns 1 and 2. The telescope the data were taken with is indicated in Column 3 (adopting the naming convention used in Table 2), magnitudes and associated errors for *JHKLM* bands given in Columns 4–8. All data are quoted in the Johnson filter system. Mean values for pre-outburst (1990–94) and post-outburst data are also indicated.

| Date | J.D. -2450000 | Source | J | H | K | L | M |
|--------------|------------------|--------|-----------|-----------|-----------|-----------|-----------|
| Mean 1990–94 | - | - | 7.6 | 6.2 | 5.0 | - | - |
| 19/08/98 | 1045.55 | CL-SAI | 7.29±0.03 | 5.77±0.03 | 4.73±0.03 | 3.13±0.02 | 2.46±0.08 |
| 22/08/98 | 1048.45 | T-Sh | 7.25±0.11 | 5.78±0.04 | 4.56±0.04 | - | - |
| 25/08/98 | 1051.46 | T-Sh | - | 5.97±0.01 | 4.69±0.01 | - | - |
| 26/08/98 | 1052.56 | SPb | 7.26±0.03 | 5.78±0.02 | 4.60±0.03 | 2.96±0.03 | 2.31±0.04 |
| 04/09/98 | 1061.48 | SPb | 7.45±0.07 | 5.76±0.03 | 4.77±0.03 | 2.97±0.04 | 2.55±0.11 |
| 08/09/98 | 1065.48 | SPb | 7.23±0.03 | 5.92±0.04 | 4.52±0.02 | 2.87±0.04 | 2.62±0.10 |
| 10/09/98 | 1067.58 | SPb | 7.32±0.06 | 5.92±0.03 | 4.59±0.05 | 3.03±0.06 | 2.42±0.06 |
| 11/09/98 | 1068.57 | SPb | 7.16±0.05 | 5.87±0.04 | 4.53±0.01 | 2.96±0.01 | 2.51±0.04 |
| 16/09/98 | 1073.60 | SPb | - | - | 4.53±0.04 | 2.86±0.04 | - |
| 27/10/98 | 1114.58 | TCS | 7.16±0.01 | 5.68±0.01 | 4.36±0.01 | - | - |
| 27/10/98 | 1114.74 | TCS | 7.30±0.01 | 5.81±0.01 | 4.52±0.01 | - | - |
| 28/10/98 | 1115.58 | TCS | 7.19±0.01 | 5.70±0.01 | 4.37±0.01 | - | - |
| 16/12/98 | 1164.47 | CL SAI | 7.11±0.01 | 5.65±0.01 | 4.44±0.01 | 2.90±0.02 | 2.43±0.04 |
| 28/12/98 | 1176.32 | CL SAI | 7.15±0.01 | 5.69±0.01 | 4.49±0.01 | 2.93±0.01 | 2.52±0.02 |
| 01/01/99 | 1180.34 | CL SAI | 7.05±0.01 | 5.60±0.01 | 4.42±0.01 | 2.88±0.02 | 2.49±0.01 |
| 20/01/99 | 1199.28 | CL SAI | 7.06±0.01 | 5.57±0.01 | 4.36±0.01 | 2.87±0.02 | 2.34±0.02 |
| 26/01/99 | 1205.26 | CL SAI | 7.07±0.01 | 5.61±0.01 | 4.39±0.01 | 2.86±0.01 | 2.51±0.02 |
| 09/03/99 | 1247.16 | T-Sh | 6.73±0.05 | 5.38±0.01 | 4.19±0.01 | - | - |
| 27/07/99 | 1387.72 | TCS | 7.03±0.02 | 5.53±0.02 | 4.07±0.02 | - | - |
| 28/07/99 | 1388.74 | TCS | 7.01±0.02 | 5.51±0.02 | 4.07±0.02 | - | - |
| 29/07/99 | 1389.74 | TCS | 7.07±0.02 | 5.57±0.02 | 4.10±0.02 | - | - |
| 01/8/99 | 1392.72 | TCS | 7.10±0.03 | 5.58±0.03 | 4.11±0.02 | - | - |
| 29/08/99 | 1420.56 | CL SAI | 7.04±0.01 | 5.64±0.01 | 4.30±0.01 | 2.71±0.02 | 2.49±0.02 |
| 25/09/99 | 1447.52 | CL SAI | 7.07±0.01 | 5.62±0.01 | 4.30±0.01 | 2.70±0.01 | 2.40±0.02 |
| 02/10/99 | 1454.56 | TCS | 7.09±0.02 | 5.57±0.02 | 4.08±0.02 | - | - |
| 03/10/99 | 1455.69 | TCS | 7.06±0.02 | 5.53±0.02 | 4.06±0.02 | - | - |
| 04/10/99 | 1456.67 | TCS | 7.15±0.03 | 5.61±0.03 | 4.12±0.02 | - | - |

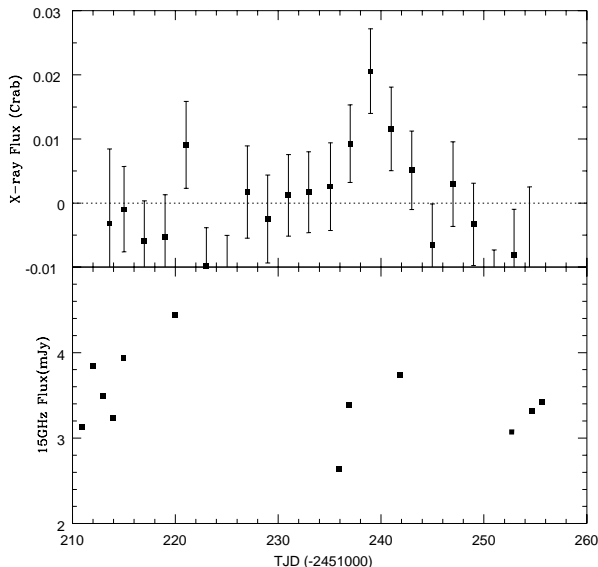


Fig. 6. 20–100 keV flux as measured by BATSE (top panel) and 15 GHz radio flux (Ryle Telescope) for the period of the possible second X-ray flare. Note that there is no indication of a corresponding flare in the (sparse) radio lightcurve.

with a typical daily 3 sigma sensitivity of better than 100 mCrab. Detector counting rates with a timing resolution of 2.048 seconds were used for the data analysis. To produce the CI Cam light curve shown in Fig. 6, single step occultation data were taken using a standard Earth occultation analysis technique used for monitoring hard X-ray sources (Harmon et al. 1992). Interference from known bright sources were removed. Based on the spectral analysis of the initial outburst in the BATSE data (Harmon et al. 1998) a photon spectral index of -3.7 was used. The single occultation step data were then fit with a power law with this index to determine flux measurements for two day averages of the data in the 20–100 keV band.

During this period the 15 GHz radio flux continued to slowly decline (eg Figs. 5 and 6), and although there appeared to be an increase in the 8 GHz flux density as measured by the GBI, we discount this increase as discussed in Sect. 3.2. Unfortunately, photometric data at this time is somewhat sparse. An *RI* broadband photometric observation of CI Cam on 1999 March 8 is suggestive of increased emission at this time; however given the difficulty in defining a “quiescent” flux it is difficult to determine if this is associated with the X-ray activity. *JHK* photometry obtained on the same date shows the system to be in a bright state, but it appears likely that this could be the result of the general trend to increasing near-IR luminosity evident at this time.

5. Discussion

Galactic B[e] stars are a rather heterogeneous class of objects first identified by Allen & Swings (1976). These authors further divided this new class of emission line object into 3 groups, based on their spectral morphology. However, the nature

of many of the galactic B[e] stars, (especially those of Allen & Swings Group 2, displaying numerous low-excitation Fe II lines) is not yet known. A distinct class of stars which show observational features similar to those of the galactic Group 2 B[e] stars was identified by Zickgraf et al. (1986) in the Magellanic Clouds (MC), consisting of high-luminosity ($\geq 10^5 L_{\odot}$) evolved objects. Lamers et al. (1998) proposed a series of sub-classifications for B[e] stars based on *both* their spectral morphology and evolutionary status (since several different types of object share the observational properties of B[e] stars). Difficulties arise in classifying galactic B[e] stars due to uncertainties in determining distances and hence luminosities. CI Cam, classified by Allen & Swings as a Group 2 object, has been proposed as the first B[e] star identified as a mass donor in a High Mass X-ray Binary (henceforth HMXB; Clark et al. 1999, B99). Below we try to estimate the luminosity and distance to CI Cam in order to find its place in the B[e] star classification scheme of Lamers et al.

Zorec (1998) and B99 both estimate that CI Cam is at a distance of ~ 2 kpc, with *interstellar* $E(B - V) \sim 0.80$ (and a large contribution to the total extinction from material local to the system). We derive a further estimate of the interstellar extinction to CI Cam of $E(B - V) = 0.65 \pm 0.2$ from analysis of the diffuse interstellar bands (DIB) present in a WHT optical spectrum (Clark et al., 2000). Assuming an average extinction curve ($R_V = 3.1$), this corresponds to an interstellar $A_v = 2.0 \pm 0.6$. Making the further assumption that the average extinction-distance relation of Neckel et al. (1980) for the region of CI Cam is applicable, the inferred distance is ~ 0.6 – 2.0 kpc, implying an upper limit to luminosity of $\sim 10^{4.8} L_{\odot}$; consistent (to within a factor of 2) with those derived by both Zorec (1998; $L \sim 10^{4.7} L_{\odot}$) and B99 ($L \sim 10^{4.9} L_{\odot}$). We therefore adopt an interstellar $E(B - V) = 0.80$, a distance of 2kpc and a mean luminosity of $\sim 10^{4.8} L_{\odot}$ for the rest of the paper.

This value is consistent with the ‘classification’ of CI Cam as an unclassifiable or unclB[e] star, according to the criteria of Lamers et al. (1998). This classification is reserved for those stars showing the B[e] phenomenon but having an uncertain evolutionary state. Clearly, the presence of an evolved companion to CI Cam demonstrates that it is likely that it is in a post Main Sequence (MS) stage of its evolution; indeed it is only marginally less luminous than the evolved supergiant B[e] (sgB[e]) stars first identified in the MC by Zickgraf et al. (1986; see above). Recently Gummertsbach et al. (1995) have suggested that the B[e] phenomenon in the MC extends down to lower ($\sim 10^4 L_{\odot}$) luminosities; it is possible that CI Cam represents a galactic counterpart to such lower luminosity MC stars. Indeed, once such evolved low luminosity ($\sim 10^{4.86} L_{\odot}$) galactic B[e] star has already been identified in the young cluster Wd 1; the unusual star Ara C (Clark et al. 1998). However, a suggestion of Miroshnichenko et al. (1999) that the galactic Group 2 B[e] stars are post-MS binary systems, which are similar to MS Be/X-ray binaries but with longer orbital periods, can not be ruled out.

5.1. Photometric variability

5.1.1. Pre-outburst variability

Pre-outburst variability in CI Cam appears to be characterised by ~ 0.4 mag. variations in all wavebands over timescales of days–weeks. As shown in Fig. 2, the variations of the broadband *UBVRI* fluxes are not correlated with corresponding changes in colour index. The situation becomes more complicated when the near-IR data is considered. As can be seen from Fig. 3, there is no correlation between the *K* band and $(J - K)$ colour index, and only a slight correlation (in the sense that the system becomes redder as it brightens) between *K* and $(H - K)$. However, when the *HK* magnitudes are compared to the *U* to *J* band data it is found that as the system brightens at shorter wavelengths there is no corresponding change in the *HK* fluxes, indicating that the system becomes bluer at this time (plots not shown for reasons of brevity). This behaviour is suggestive of two distinct emission components varying independently of one another. Possible sources of variability in the system include thermal dust emission at longer wavelengths and free–free/ free–bound (*f–f–b*) wind emission at shorter wavelengths (see below).

Unfortunately, only limited long term monitoring of other galactic B[e] stars has been undertaken. Of the small number of candidate B[e] stars that have been the subject of such observations, most have shown only a low degree of photometric variability. Exceptions include the MC binary system R4 ($\Delta V \sim 0.7$ mag; Zickgraf et al. 1986) and the galactic stars HD 87643 (which faded by ~ 1 mag since the 1960’s), and MWC 342 ($\Delta V \sim 0.6$ mag). Of these, only HD 87643 showed a long term trend in colour with brightness, becoming redder as it faded (Miroshnichenko 1998).

5.1.2. Outburst variability

The 1998 April outburst is clearly of a very different character from the variability observed during quiescence, almost certainly as a result of interaction between the compact companion and the dense circumstellar environment of CI Cam. Possible sources of excess continuum emission during the X-ray outburst include increased *f–f–b* emission from an enhanced wind with a larger mass loss rate (*M*), X-ray heating of the primary and/or circumstellar envelope, thermal reradiation from the dust cloud and synchrotron (and possible *f–f–b*) emission from the ejecta responsible for the radio flux. Additionally, given the rich emission line spectrum, the contribution of line emission to the broadband photometry is likely to be non-negligible; this will be quantified in Clark et al. (2000).

B99 remark on the similarity between the HMXB system A0538-66 and CI Cam, and suggest that the optical-near IR flaring in CI Cam may have the same origin as seen in A0538-66. During outburst A0538-66 is observed to brighten by up to ~ 2.5 mag. in the optical, and also become significantly bluer; Densham et al. (1983) interpret this as being due to reprocessing of X-rays by the gaseous circumstellar envelope of the Be star primary. Despite the similarities between the optical and X-ray e-folding timescales for CI Cam, F98 exclude reprocessing of X-rays as a cause of the optical flaring as they find from

their data that the $(V - R)$ colour index remains \sim constant throughout the outburst. However, it is clear from our data that this is incorrect; CI Cam was significantly redder during outburst, becoming bluer as it faded (Fig. 2), suggesting that the extra emission component is cooler than the stellar temperature. Given that thermal emission from hot dust inferred by B99 is unlikely to contribute much flux at such short wavelengths it appears more likely to come from a combination of line and continuum emission from hot gas, either a result of X-ray heating of the circumstellar envelope, or due to an increased mass loss rate (which might have acted to trigger the outburst). However, without photometric observations of the system before the X-ray outburst, or orbital parameters for the compact object we are unable to distinguish between these scenarios.

We note that this relationship is *not* seen for the *U* band; the $(U - B)$ index remains \sim constant throughout the outburst. Whether or not this indicates emission from a further hot, blue body within the system is at present unclear. B99 present *JHK* spectra of CI Cam obtained shortly after the X-ray flare indicating that there was also a substantial increase in the near-IR flux, which they attribute to X-ray heating of the circumstellar dust. Although it is likely that at least some of the near-IR flux originates in a greater contribution from the gaseous component of the circumstellar envelope, this observation supports our general conclusion that the optical flaring is most likely a result of reradiation of the X-ray flux.

5.1.3. Post-outburst variability

Significant post-outburst variability is observed in data longwards of the *V* band, and appears to arise from two different sources, given the lack of correlation between the *RI* and *JHK* bands. We tentatively attribute this emission to two different mechanisms; thermal (*f–f–b* and recombination line) emission from a gaseous component of the circumstellar envelope responsible for the increased emission in the *R* and *I* band (Sect. 5.3), and a combination of *f–f–b* and increased emission from hot dust at longer wavelengths (Sect. 5.2). The apparent decrease in the *RI* band emission after 1998 December could arise from a number of different causes; a decrease in either the ionising radiation flux or the emission measure of the circumstellar envelope, or an increase in the temperature of the emitting material. Analysis of contemporaneous optical spectra of the source may help us to distinguish between these possibilities. The steady increase of the near IR flux is suggestive of the formation of new, hot dust at the inner edge of the envelope; this is discussed in Sect. 5.2.

The increased hard (BATSE) X-ray activity observed between 1999 February 22–March 7 differs considerably from that observed during the 1998 April flare. The X-ray luminosity is much lower, peaking at only ~ 30 milliCrab, compared to a flux in excess of 1 Crab at the peak of the 1998 April flare. Equally, the 1998 flare was far more rapid (rise time of ~ 0.1 days and an e-folding decay timescale of 0.56 days) compared to the 1999 flare (lasting for a total of ~ 6 days). No associated flaring comparable to that observed in the 1998 April outburst was

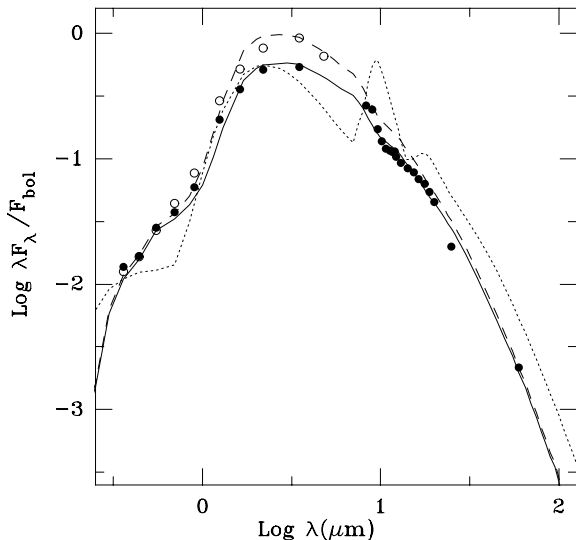


Fig. 7. Results of the DUSTY model fits to the un-reddened pre-outburst (solid circles) and post-outburst (open circles) optical-IR SED of CI Cam. The dotted line represents a best fit to the pre-outburst data assuming a MRN dust composition (no fit was attempted to the post-outburst data). Solid and dashed lines represent best fits to the pre- and post-outbursts data respectively, assuming dust composed of amorphous carbon.

observed at other wavelengths, suggesting the outburst was not sufficiently energetic to produce an impulsive ejection of material, as was inferred for the 1998 outburst (Mioduszewski et al. in prep.).

5.2. The dusty envelope of CI Cam

Given the increasing post-outburst IR excess of CI Cam, we have used the radiative transfer code DUSTY (Ivezić, Nenkova & Elitzur 1999) to investigate changes in the physical properties of the dusty envelope over time. The code solves the radiation transfer problem for spherical dusty envelopes, calculating the dust temperature distribution self-consistently and controlling flux convergence at different radii in the envelope.

The pre-outburst quiescent SED was constructed from the averaged *UBVR IJHKL* photometry of Bergner et al. (1995), 12–60 μm IRAS fluxes, and an IRAS LRS spectrum. The LRS spectrum was noisy, and so we averaged over every 4 consecutive points, and smoothed the resultant spectrum using the Savitsky-Golay method (Press et al. 1992). The post-outburst SED was constructed from the averaged *UBVR IJHKL* data obtained in 1998. Stellar radiation was described by a Kurucz (1994) model for $T_{\text{eff}}=30,000$ K and $\log g=3.5$ (the exact value was found to have a negligible effect on the emergent SED). We computed the SED for two different types of circumstellar dust; interstellar dust (MRN mixture: Mathis, Rumble, Nordsieck 1977) and amorphous carbon (Hanner 1988); in each case a single power law density gradient of the form r^{-p} was adopted.

For both of the dust types a large number of models with different parameters were calculated, and the emergent theoretical SEDs were compared to the observed pre-outburst data, after the addition of a second component of reddening attributed to interstellar extinction, and calculated from the interstellar extinction law of Savage & Mathis (1979). When fitting the post-outburst data the interstellar extinction was fixed at the best-fit value from the pre-outburst data modelling. The best fits to the data were determined using the weighted least square method.

The results of the modelling are presented in Fig. 7. We find that the envelope made of the MRN dust should have a large optical depth (of the order of 1.5 in the optical region) and a much smaller interstellar extinction than observed. The synthetic spectrum also displays noticeable silicate emission features at 9.7 and 18 microns which do not appear to be present in the IRAS LRS spectrum. However, changing the average grain size by removing the smaller grains will reduce the strength of the emission features; considering the ease with which CI Cam can eject smaller grains (see below), this is perhaps an attractive proposition. The envelope made of carbon dust gives a featureless IR spectrum and has a small optical depth, that requires a rather large interstellar extinction (or another local source of reddening) in order to fit the observed SED; indeed it is somewhat in excess of that derived from analysis of the optical spectra (see Sect. 5.0).

Best fit model parameters for the carbon dust include $T_{\text{in}}=1500$ K, $A_v=3.71$ mag., $T_{\text{out}}=110$ K, $Y_{\text{out}}=1000$ and the density distribution power law index $p=1.75$ for both the quiescent pre- and post-outburst SED of CI Cam. Here T_{in} and T_{out} are the temperature at the inner and outer edges, A_v the extinction to the system (initially assumed to be of interstellar origin) and Y_{out} the ratio of the outer and inner envelope radii. The best fit parameter sets differ only in τ_v (the overall optical depth of the envelope), which is 0.06 for the pre- and 0.09 for the post-outburst SED, respectively; consistent with the production of new dust. We note that Waters et al. (1998) found amorphous carbon dust around the binary sgB[e] star GG Carinae, with a SED compatible with an r^{-2} density gradient, similar to that found for CI Cam, and Bjorkman (1998) also found amorphous carbon dust to be present around the MC sgB[e] star R126.

However, caution must be applied to the results of these models, due to the uncertainty in the geometry and composition of the circumstellar envelope around CI Cam. Changing the geometry of the envelope can act to produce a featureless mid-IR spectrum; for instance an optically thick-disc like envelope would also produce such a spectrum. Such a disc-like geometry is attractive, as it has previously has been suggested for the MC sgB[e] stars (Zickgraf et al. 1986). However, since a hot, stellar component is present in the SED of CI Cam, such an optically thick disc must also be both geometrically thin and seen almost edge on so that it produces little obscuration of the stellar disc, and an additional source of extinction or reddening close to the system is then required, since only $A_v=2.1$ can be explained by the interstellar component of extinction (Sect. 5.0).

The chemical composition and grain size in CI Cam are also uncertain, due to the lack of high quality IR spectroscopy. Typ-

ically, the dust around the broad class of B[e] stars is found to be a mixture of olivines (~ 60 per cent), FeO (~ 30 per cent) and a small amount of C rich material (van den Ancker, private communication), although B[e] stars are a very heterogeneous class of object, with some stars (eg GG Carinae) showing substantially different dust chemistries. Indeed, changes in the composition of the dust due to X-ray irradiation could lead to changes in the emissivity, and hence SED. However, given that this would be an impulsive event, this scenario appears unlikely in the light of the gradual increase in near-IR flux over the course of ~ 9 months.

If the conclusion that additional dust has formed in the aftermath of the flaring episode is correct, one can ask where and how it was formed, given that dust formation in hot stellar winds requires high densities at sufficiently large radii to permit the dust to condense. From Eq. (15) of Bjorkman (1998), and adopting a dust condensation radius of 5.3×10^{12} m, we find that for a spherical wind with a uniform mass loss rate, we need an unrealistically high \dot{M} to allow dust condensation (assuming the terminal velocity of the wind $V_\infty > 100 \text{ km s}^{-1}$, typical for hot, luminous stars),

$$(\dot{M}/10^{-7} M_\odot) = 25(V_\infty/30 \text{ km s}^{-1}) \quad (2)$$

suggesting instead that dust either forms in a circumstellar disc or in dense shells of ejecta, possibly resulting from shocks in the wind. The episodic dust formation observed in some WR-O star binary systems is thought to occur in shocked regions caused by the colliding winds of the two luminous components (eg WR 125 and WR 19; Williams et al. 1994 and Veen et al. 1998 respectively); since radio maps provide evidence for the formation of an expanding shell of ejecta following the outburst (Mioduszewski et al., in prep), it is tempting to speculate that the dust formed may be associated with this region.

The suggestion of episodic (or quasi-continuous) dust formation is also consistent with the claim of B99 that the dust shell around CI Cam appears to be composed of comparatively large particles ($> 0.3 \mu\text{m}$), which they attribute to radiation pressure removing the smaller particles. Assuming a luminosity of $\sim 10^5 L_\odot$ and a mass of $\sim 20 M_\odot$ (Zorec 1998), we can apply the analysis of Sitko et al. (1994) to CI Cam. From Eq. (2) of Sitko et al. (1994), under the assumption of weak coupling between dust and gas, we find that it is very easy for CI Cam to eject grains of radius $0.3 \mu\text{m}$ or less (indeed much larger grains would also be ejected). Even with a strong coupling between gas and dust (such that the radiation field had to eject both dust and gas) we find that the radiation field of CI Cam would still be able to efficiently accelerate particles of sizes $\sim 1 \mu\text{m}$ or larger. Since dust particles of this size are inferred to be present, it appears likely that the dust is being continually replenished within the system.

5.3. Emission from a gaseous envelope

Modelling the SED of CI Cam, we determine a colour excess, $E(B - V) \sim 1.1$ mag. However we determine an interstellar $E(B - V) \sim 0.8$ (Sect. 5.0), indicating that additional circum-

stellar extinction or reddening exists. Possible sources include circumstellar dust extinction (which for dust composed of amorphous carbon we find to be small; Sect. 5.2) or f-f/f-b emission (a contribution from which is not included in the model results presented in Sect. 5.2). If CI Cam is surrounded by a gaseous disk (the Balmer line profiles indicating a non-spherical distribution of the gaseous component; Clark et al. 2000) with a structure similar to that inferred for *classical* Be stars, reddening from the gaseous envelope may reach values as high as $E(B - V) \sim 0.3$; such values would also imply significant emission, which may contribute as much as $\Delta V \sim 1$ mag (these values being obtained in the framework of an isothermal Be disk-like model similar to that described by Waters et al. 1987). Note that true sgB[e] stars are also expected to have dense gaseous circumstellar discs that are also likely to contribute a significant amount of f-f emission; however to date this contribution has yet to be accurately quantified.

Under the assumption of an ionised, constant velocity isothermal wind we can derive upper limits to (\dot{M}/V_∞) from the non-detection of f-f/f-b emission at 1.4 GHz using Eq. (1) of Leitherer et al. (1995)

$$S_\nu = 2.32 \times 10^{-4} \left(\frac{\dot{M}Z}{V_\infty \mu} \right)^{4/3} \left(\frac{\gamma g_\nu \nu}{d^3} \right)^{2/3} \quad (3)$$

where S_ν is the flux density in mJy, ν the frequency in Hz, d the distance in kpc (2kpc; Sect. 5); \dot{M} is given in units of $10^{-6} M_\odot \text{ yr}^{-1}$ and V_∞ in units of 100 km s^{-1} . μ , Z , γ are the mean molecular weight, the rms ionic charge and the mean number of electrons per ion respectively; we adopt the values given by Leitherer et al. (1995) for the B stars in their sample for CI Cam. The free-free Gaunt factor, g_ν was calculated with Eq. (3) of Leitherer et al. (1995), adopting a value for T_e , the electron temperature of the wind appropriate for the B stars in Leitherer et al. (1995), noting that g_ν only has a weak dependence on T_e . The upper limit to the 1.4 GHz flux of $\sim 1 \text{ mJy}$ therefore implies

$$(\dot{M}/V_\infty) < 3.48 \quad (4)$$

When compared to the lower limits to (\dot{M}/V_∞) implied for dust condensation in a spherical wind we find that CI Cam would have been detected at 1.4 GHz if the wind density was sufficiently high to permit dust to form, strengthening the case for dust formation in a equatorial disc or shocked ejecta. We note that the 1.4 GHz flux estimates assume that the wind is *completely* ionised; if the wind in CI Cam is not fully ionised then (\dot{M}/V_∞) could exceed the value given.

6. Summary

We have presented long term photometric observations of CI Cam, the proposed counterpart to the X-ray transient XTE J0421+560 before, during and after the 1998 April X-ray flare. We find evidence for photometric variability in pre-outburst, outburst and post-outburst datasets. Pre-outburst rapid variability is characterised by variability of ~ 0.4 mags. in all wavebands; there is no indication of significant flaring in these data.

During and immediately after the X-ray flaring *UBVRI* broadband photometry clearly indicates a substantial brightening at all wavelengths. Although near-IR photometry was not available, *JHK* spectra obtained during the outburst suggest that the system had also undergone flaring in the near-IR as well (B99). Multiwavelength radio observations at this time show a corresponding radio flare which appears to evolve according to the behaviour expected for expanding, synchrotron emitting ejecta. Subsequent long term monitoring of the 15 GHz radio flux shows a monotonic decay for the ~ 18 months following the 1998 X-ray flare. BATSE 20–100 keV observations suggest a possible second X-ray flare (of significantly smaller magnitude than the 1998 April outburst) around 1999 March 2; however no indication of a corresponding radio or optical flare was observed. If the second BATSE outburst is due to another pass by the compact companion through the circumstellar envelope then the time interval between the two outbursts (~ 335 days) reflects the orbital period (or some multiple of it).

Post-outburst photometry showed that CI Cam was significantly brighter at longer wavelengths than in the pre-outburst state, and continued to brighten in the near-IR, indicating differing emission mechanisms for the optical-near IR and radio fluxes. We tentatively attribute this increase in emission to a combination of $f-f-b$ emission from a gaseous component of the circumstellar envelope (*R* & *I* bands) and increased emission from a hot dust component (*JHKLM* bands). Using the DUSTY code of Ivezić we model both pre- and post-outburst data, and find that there appears to have been an episode of dust formation at the inner edge of the dusty envelope. We note however, that these results are subject to significant uncertainty due to the poor quality of the IR spectroscopy used to constrain the dust chemistry of the envelope. We reject the hypothesis of a change in dust composition due to X-ray irradiation since this would lead to an impulsive change in the near-IR emission while we observe a general increase in near-IR flux over a period of ~ 1 year. Likewise we find no evidence for continued X-ray emission from the compact object that could be responsible for the increased near-IR flux via reprocessing in the pre-existing dusty envelope. However, we find a discrepancy between the reddening to the system inferred from the DIB, and that derived from the modelling, suggesting a second source of reddening local to the system, which we suspect may arise from $f-f-b$ emission from hot gas in the circumstellar envelope. However, further discussion must await higher quality IR spectroscopic observations to determine the dust composition so that more accurate modelling of the SED of CI Cam can be undertaken.

Acknowledgements. The Green Bank Interferometer is a facility of the National Science Foundation operated by the NRAO in support of NASA High Energy Astrophysics programs. Quick look ASM results provided by the ASM/RXTE team. The Ryle Telescope is supported by PPARC. Larionov acknowledges financial support from the Russian Federal Program ‘Integration’, grant number K0232. We gratefully acknowledge the work of the many observers contributing to VSNET. We wish to thank J. Telting, M. Lehnert and Y. Simis for obtaining prompt JKT photometry so soon after the initial X-ray detection. We

also thank I.A. Steele, R.P. Fender and M. van Ancker for stimulating discussions.

References

- Allen D.A., Swings J.P., 1976, *A&A* 47, 293
 Altenhoff W.J., Braes L.L.E., Olton F.M., Wendker H.J., 1976, *A&A* 46, 11
 Belloni T., Dieters S., van der Ancker et al., 1999, *ApJ*, accepted (B99)
 Bergner Yu.K., Bondarenko S.L., Miroshnichenko A.S., et al., 1988, *Izvestia Glavn. Astron. Observ. v Pulkove* 205, 142
 Bergner Yu.K., Miroshnichenko A.S., Yudin R.V., et al., 1995, *A&AS* 112, 221
 Bjorkman J.E., 1998, In: Jaschek, C., Hubert, A.M. (eds.), *B[e] stars*. A.M. Kluwer Academic Publishers, p. 189
 Clark J.S., Fender R.P., Waters L.B.F.M., et al., 1998, *MNRAS* 299, L43
 Clark J.S., Steele I.A., Fender R.P., Coe M.J., 1999, *A&A* 348, 888
 Clark J.S., et al., 2000, in prep.
 Densham R.H., Charles P.A., Menzies J.W., et al., 1983, *MNRAS* 205, 1117
 Downes R.A., 1984, *PASP* 96, 807
 Fishman G.J., et al. 1989, In: N. Johnson (ed.), *Proc. Gamma-Ray Observatory Science Workshop, Greenbelt: Goddard Space Flight Center*, p. 2-39
 Frontera F., et al., 1998, *A&A* 339, L69 (F98)
 Garcia M.R., Berlind P., Barton E., McClintock J.E., 1998, *IAUC* 6865
 Goranskii V.P., Lyuty V.M., Metlova N.V., 2000, *Astron. Zhurn.*, in press
 Gregory P.C., Condon J.J., 1991, *ApJS* 75, 1011
 Gummertsbach C.A., Zickgraf F.-J., Wolf B., 1995, *A&A* 302, 409
 Hanner M.S., 1988, *Infrared Observations of Comets Halley and Wilson and Properties of the Grains (NASA89-13330)*, 22
 Harmon B.A., et al. 1992, in: *Proc. Compton Observatory Science Workshop, C.R. Shrader, N. Gehrels, B. Dennis (eds.)*, Washington: NASA, 69
 Harmon B.A., Fishman G.J., Pasciasas W.S., 1998, *IAUC* 6874
 Hjellming R.M., Mioduszewski A.J., 1998a, *IAUC* 6857
 Hjellming R.M., Mioduszewski A.J., 1998b, *IAUC* 6862
 Ivezić Ž., Nenkova M., Elitzur M., 1999, *User Manual for DUSTY, Internal Report, University of Kentucky*, accessible at <http://www.pa.uky.edu/~moshe/dusty/>
 Kurucz R.L., 1994, *Smithsonian Astrophys. Obs.*, CD-ROM No. 19
 Lamers H.J.G.L.M., Zickgraf F.-J., de Winter D., et al., 1998, *A&A* 340, 117
 Leitherer C., Chapman J.M., Koribalski B., 1995, *ApJ* 450, 289
 Marshall F.E., Strohmayer T.E., 1998, *IAUC* 6857
 Mathis J.S., Rumpl W., Nordsieck K.H., 1977, *ApJ* 217, 425 (MRN)
 Miroshnichenko A.S., 1995, *Astronomical & Astrophysical Transactions* 6, 251
 Miroshnichenko A.S., 1998, In: Jaschek C., Hubert A.M. (eds.), *B[e] stars*, Kluwer Academic Publishers, p. 145
 Miroshnichenko A.S., Corporon P., Shejkina T.A., 1999, *BAAS* 31, 845
 Neckel Th., Klare G., Sarcander M., 1980, *A&AS* 42, 251
 Orr A., Parmar A. N., Orlandini M., Frontera F., Dal Fiume D., Segreto A., Santangelo A., Tavani M., 1998, *A&A* 340, 190
 Piirola V., 1988, In: ‘‘Polarized radiation of circumstellar origin’’, edited by Coyne G.V., Magalhães A.M., Moffat A.F.J., Schulte-Ladbeck R.E., Tapia S., Wickramasinghe D.T., *Vatican Observatory – Vatican City State*, p. 735

- Pooley G.G., Fender R.P., 1997, MNRAS 292, 925
- Press W.H., Teukolsky S.A., Vetterlink W.T., Flannery B.P., 1992, in: Numerical recipes in Fortran. the art of Scientific Computing, Cambridge Univ. Press
- Robinson E.L., Welsh W.F., Adams M.T., Cornell M.E., 1998, IAUC 6862
- Savage B.D., Mathis J.S., 1979, ARA&A 17, 73
- Sitko M.L., Halbedel E.M., Lawrence G. F., et al., 1994, ApJ 432, 753
- Smith D., Reillard R., Swank J., et al., 1998, IAUC 6855
- Telting J.H., Waters L.B.F.M., Roche P., et al., 1998, MNRAS 296, 785
- van der Laan H., 1966, Nat 211, 1131
- Veen P.M., van der Hucht K.A., Williams P.M., et al., 1998, A&A 339, L45
- Vessey S.J., Green D.A., 1998, MNRAS 294, 607
- Wagner R.M., Starrfield S., Shrader C., et al., 1998, IAUC 6924
- Waltman E.B., Fiedler R.L., Johnston K.J., Ghigo F.D., 1994, AJ 108, 179.
- Waters L.B.F.M., Cote J., Lamers H. J.G.L.M., 1987, A&A 185, 206
- Waters L.B.F.M., Morris P.M., Voors R.H.M., Lamers H.J.G.L.M., 1998, In: Hubert A.M., Jaschek C. (eds.), B[e] Stars, Dordrecht: Kluwer, p. 111
- Woodsworth A.W., Hughes V.A., 1977, A&A 58, 105
- Williams P.M., van der Hucht K.A., Kidger M.R., et al., 1994, MNRAS 266, 247
- Ueda Y., Ishida M., Inoue H., et al., 1998, ApJ 508, 167
- Zickgraf F.-J., Wolf B., Leitherer C., et al., 1986, A&A 163, 119
- Zorec J., 1998, In: Hubert A.M., Jaschek C. (eds.), B[e] Stars, Dordrecht: Kluwer, p. 27